COMPUTATIONAL CONTINUUM MECHANICS

ВЫЧИСЛИТЕЛЬНАЯ МЕХАНИКА СЛОШНЫХ СРЕД

Computational Continuum Mechanics. 2021. Vol. 14. No. 1. pp. 77-90 DOI: 10.7242/1999-6691/2021.14.1.7

THE INFLUENCE OF CHEMICAL REACTION PARAMETERS ON THE INTERACTION OF THERMAL, DIFFUSION AND MECHANICAL WAVES UNDER SURFACE TREATMENT BY A PARTICLE BEAM

E.S. Parfenova and A.G. Knyazeva

Institute of Strength Physics and Materials Science SB RAS, Tomsk, Russian Federation

A coupled non-isothermal model of the penetration process of a material into a target surface under conditions of surface treatment with a particle beam is presented. The model takes into account the interaction of impurity diffusion, heat propagation, mechanical disturbances and the chemical reaction between the introduced impurity and the substrate material. The problem is formulated in terms of dimensionless variables. All model parameters and the range of numerical values are given. The problem is solved numerically using an implicit symmetric difference scheme of the second order approximation in time and coordinates. The solutions are obtained for different time intervals determined by the characteristic pulse action time and relaxation times for diffusion and thermal conductivity. It has been established that the interrelation of processes of different scales leads to the appearance of distortions on strain and stress waves, and the distributions of temperature and impurity concentration acquire a wave character. The formation of chemical compound leads to a decrease in the concentration of impurities and to an increase in temperature, stresses and deformation. It is shown that the chemical reaction at low heat generation proceeds only as long as the temperature increases due to the introduced energy. It has been found that, at slow formation of the product in the reaction, the chemical interaction practically does not affect the propagation of temperature, deformation, stresses and impurity concentration.

Key words: coupled model, particle beam, wave propagation, nonlinear effects, elastic stresses, diffusion, heat conduction, relaxation of heat flux, relaxation of mass flux, chemical reaction

1. Introduction

Surface treatment of metals by a charged particles beam is a long-estableshed method of processing materials to improve their mechanical properties and wear resistance and, consequently, to increase the service life of of various mechanical products in engineering machine-building [1, 2]. In particular, solid solutions formed as a result of introduction of particles into the surface layers impede the dislocation movement, as well as the nucleation and propagation of microcracks. This significantly increases the mechanical and tribotechnical characteristics of the materials [3]. There are a lot of physical and chemical processes when flux particles interact with the treated surface. The particles of the flow collide with the surface, and some physical and chemical processes interact with each other and affect the final result. For example, in [4, 5] it was found that surface modified layers are formed containing fine-dispersed intermetallic phases and solid solutions of variable composition in depth form after high-intensity ion implantation. Also the relationship was found between the structural phase state of the modified materials and the implantation conditions.

It was noted in [6] that the impact of the particle flux on the target leads to its heating, the appearance of shock waves and ablation of the material from the treated surface. It was determined that thermal and barodiffusion processes are responsible for the mass transfer of introduced particles in the surface layers, while at depth the main contribution is made by the shock wave. The duration of action, flux parameters and material composition primarily influence on the depth of the modified layer and on the nature of the structural-phase transformations in it [7]. Thus, it would seem that by controlling the external processing parameters one can achieve maximum results in improving the surface properties, but insufficient understanding of the physical processes occurring in the solid during treatment limits the possibilities of this method despite the available experimental and theoretical material. Therefore, research in this area is relevant.

Mathematical modeling makes it possible to study in detail co-occuring processes relating with surface treatment by a particle flux. First, when building a model and performing a parametric study, one can select only the phenomena of interest and discard the rest, while the experiment does not provide such an opportunity. Secondly, it is possible to track the dynamics of processes from

Email addresses for correspondence: linasergg@mail.ru

the introduction moment to later times. Third, there is no need to purchase expensive materials and equipment for the experiment.

Fourier's law is classical for describing heat transfer. However, for the cases of heat transfer in fast processes on micro-, nanoscale, the models taking into account nonlinear effects are used. A detailed review of the laws of heat conduction that do not fit into classical concepts, is given in [8]. Similar changes for nonequilibrium conditions are introduced into Fick's equations. In [9, 10] the process of harmonic disturbances propagation is studied in a thermoelastic medium, taking into account relaxation of heat flux, i.e. heat propagation obeys the hyperbolic heat conduction equation. Diffusion processes are not considered here. In [11] a model of impurity redistribution in a three-component system is discussed. The mechanical stresses occurring in the diffusion zone are taken into account. This leads to changes in the width of the diffusion zone, as well as the quality of the concentration distribution. In [12] the effect of thermodiffusion on redistribution of components and mechanical stresses in the surface layer of the material during its treatment by a particles flux was studied. It was found that thermodiffusion is most significant for the material with higher viscosity. In [13], a model of the intermetallic phase formation in the surface layer of aluminum during its modification by nickel ions was presented. Data on the preferential formation of phases for different processing conditions were obtained. However, this model does not regard the interaction of diffusion and mechanical disturbances. In [14, 15], analytical methods are used to study the problems of thermoelastic diffusion.

The aim of this work is to numerically investigate the combined propagation of elastic mechanical waves (generating by particle impact on the surface) and diffusion of introduced particles taking into consideration their chemical interaction with the treated material and the nonisothermal nature of the process. The relaxation times of the heat and mass fluxes are also considered in the mathematical model. Thus, the equations of heat conduction and diffusion do not correspond to the classical equations. In addition, in contrast to the earlier work of the authors [16], the thermal conductivity and balance equations of the introduced component take into account the source/loss of heat due to the chemical reaction and the cost of the introduced element to the formation of a chemical compound.

2. Mathematical formulation of the problem

The process of charged particles interaction with the target surface under the condition of chemical interaction of particles with the processed material can be described within the framework of the thermoelastic diffusion theory [18–20] taking into account the nonlinear effects associated with the dependence of the diffusion coefficient and the chemical reaction rate on the material composition and temperature. Suppose that the chemical reaction is possible in the surface layer and it satisfies the overall scheme:

$$\nu_B X_B + \nu_C X_C = \nu_P X_P,$$

where X_B is the base element reacting with the introduced element X_C, X_P is the reaction product, ν_B, ν_C and ν_P are stoichiometric coefficients. In the general case, the rate of such reaction can be written in the form:

$$\Phi = k_0 \left[X_C\right]^{\nu_C} \left[X_B\right]^{\nu_B} \phi(T),$$

where k_0 is the pre-exponential factor or rate constant of a chemical reaction; the concentration of the corresponding substance is indicated with square brackets. Below, to simplify the record, the square brackets are omitted and the following notations are used: C is the mass concentration of the introduced element; C_P is the mass concentration of the reaction product.

Because the kinetics of reactions in the solid phase is not obvious, for simplicity we will assume that the reaction rate is proportional to the concentration of the introduced element, and depends on the temperature according to Arrhenius law:

$$\Phi = \rho k_0 \psi(C) \exp\left(-\frac{E_R}{RT}\right).$$

Here: ρ is the density of target material; $\psi(C) = C(1-C-C_P)$ is the kinetic function; E_R is the activation energy of the chemical reaction; R is the universal gas constant. Assume that all stoichiometric coefficients are equal to one.

Then the equations system of the non-isothermal mechanodiffusion model describing the initial stage of the particle beam penetration process into target surface [16], supplemented with the chemical kinetics equation, will take the form:

$$\frac{d\rho}{dt} + \rho \nabla \cdot \mathbf{v} = 0, \tag{1}$$

$$\rho C_\sigma \frac{dT}{dt} + \alpha_T T \frac{d\sigma_{kk}}{dt} = -\nabla \cdot \mathbf{J}_q + W_{ch}, \tag{2}$$

$$\rho \frac{dC}{dt} = -\nabla \cdot \mathbf{J} - \nu_C \Phi, \tag{3}$$

$$\rho \frac{dC_P}{dt} = \nu_P \Phi, \tag{4}$$

$$\rho \frac{d\mathbf{v}}{dt} = \nabla \cdot \boldsymbol{\sigma}. \tag{5}$$

In equations (1)-(5) the following notations are taken: t is the time; T is the temperature; C_σ is the heat capacity at constant stress; α_T is the linear coefficient of thermal expansion; σ_{kk} is the first invariant of the stress tensor; $\mathbf{J}_q$ is the heat flux; W_{ch} is the source or loss of heat by chemical reaction, $W_{ch} = Q\Phi$, where Q is the thermal effect of a chemical reaction; $\mathbf{J}$ is the mass flux; Φ is the conversion rate; $\mathbf{v}$ is the mass average velocity; $\boldsymbol{\sigma}$ is the stress tensor with components σ_{ij}; $\nabla \cdot ... = \mathrm{div}(...)$. Mass forces in the equations are neglected.

The increments of the strain tensor components connect with the increments of the elastic stress tensor components, the concentration and temperature increments by the generalized relations:

$$d\sigma_{ij} = 2\mu d\varepsilon_{ij} + \delta_{ij}\left(\lambda d\varepsilon_{kk} - K d\omega\right). \tag{6}$$

Here: μ, λ are Lame coefficient (coefficient μ in linear theory coincides with the shear modulus); K is the isothermal bulk module, $K = \lambda + 2\mu/3$; ω is the temperature and concentration function,

$$\omega = 3\left[\alpha_T (T - T_0) + (\alpha - \alpha_0)(C - C_0) + (\alpha_P - \alpha_0)(C_P - C_{P0})\right];$$

α, α_P, α_0 are concentration expansion coefficients of the introduced element, the reaction product, and the base element; T_0, C_0, C_{P0} are initial temperature and initial component concentrations.

In the generalized relation for the mass flux, we take into account the transfer under the action of stresses; we assume that the relaxation times of the heat and mass fluxes are different; we will not consider the Soret and Dufaure phenomena. Then

$$\mathbf{J} = -\rho D \nabla C + B_\sigma C \nabla \sigma_{kk} - t_D \frac{d\mathbf{J}}{dt}, \tag{7}$$

$$\mathbf{J}_q = -\lambda_T \nabla T - t_q \frac{d\mathbf{J}_q}{dt}. \tag{8}$$

With that: $D = D^0 f(C)$ is the diffusion coefficient, where $D^0 = D_0 \exp\left(-E_D / (RT)\right)$ is the self-diffusion coefficient; $f(C)$ is the function that takes into account the dependence of the diffusion coefficient on the composition, where D_0 is the pre-exponent in the law for the diffusion coefficient, E_D is the activation energy for the diffusion process; $B_\sigma = D^0 m \Delta\alpha / (RT)$ is the mass transfer coefficient under the action of stresses, where m is the molar mass, $\Delta\alpha = (\alpha - \alpha_0)$ is the difference between the concentration expansion coefficients of the introduced element and the base element; t_D is the mass flux relaxation time; λ_T is the coefficient of thermal conductivity; t_q is the heat flux relaxation time. In this study $f(C) = 1$, i.e. the diffusion coefficient D is equal to the self-diffusion coefficient D^0.

Let us introduce some simplifications by analogy with the work [16]. Deformations, velocities and accelerations will be considered small. Then the need for the equation (1) disappears, and the left part of the motion equation (5) becomes the following [24]:

$$\rho \frac{d\mathbf{v}}{dt} \approx \rho_0 \left(\frac{\partial \mathbf{v}}{\partial t} + \mathbf{v} \nabla \cdot \mathbf{v} \right) \approx \rho_0 \frac{\partial^2 \mathbf{u}}{\partial t^2}.$$

Moreover, as in thermoelastic diffusion models [14, 25-27], instead of the relations in the increments (6) we can write:

$$\sigma_{ij} = 2\mu\varepsilon_{ij} + \delta_{ij}\left(\lambda\varepsilon_{kk} - K\omega\right).$$

The particle beam is considered to be uniformly distributed along the treated surface, so we can restrict ourselves to a one-dimensional problem. In this case, the condition of uniaxial loading is realized:

$$\sigma_{xx} = \sigma, \qquad \sigma_{yy} = \sigma_{zz} = 0, \qquad \sigma = E\left(\varepsilon - \frac{\omega}{3}\right), \tag{9}$$

where $\varepsilon = \varepsilon_{xx}$ and E is the elastic modulus, $E = \mu \dfrac{3\lambda + 2\mu}{\lambda + \mu}$. Because the displacements and deformations are small, the Cauchy relations take place.

As a result, we obtain a system of one-dimensional coupled equations in which the vector notations for the fluxes are replaced by scalar one:

$$\rho_0 \frac{\partial C}{\partial t} = -\frac{\partial J}{\partial x} - \Phi; \tag{10}$$

$$\rho_0 C_\sigma \frac{\partial T}{\partial t} + \alpha_T T \frac{\partial \sigma}{\partial t} = -\frac{\partial J_q}{\partial x} + Q\Phi; \tag{11}$$

$$\rho_0 \frac{\partial^2 u}{\partial t^2} = \frac{\partial \sigma}{\partial x}; \tag{12}$$

$$\rho_0 \frac{\partial C_P}{\partial t} = \Phi. \tag{13}$$

The defining relations (6)-(8) and the Cauchy relation take the form:

$$J = -\rho_0 D\frac{\partial C}{\partial x} + B_\sigma C\frac{\partial \sigma}{\partial x} - t_D\frac{\partial J}{\partial t}; \tag{14}$$

$$J_q = -\lambda_T\frac{\partial T}{\partial x} - t_q\frac{\partial J_q}{\partial t}; \tag{15}$$

$$\sigma = E\left(\varepsilon - \alpha_T\left(T - T_0\right) - \left(\alpha - \alpha_0\right)\left(C - C_0\right) - \left(\alpha_P - \alpha_0\right)\left(C_P - C_{P0}\right)\right); \tag{16}$$

$$\varepsilon = \frac{\partial u}{\partial x}. \tag{17}$$

The initial and boundary conditions for system (10)–(13):

$$\begin{gathered} x = 0: \quad J = m_0\phi(t); \quad J_q = q_0\phi(t); \quad \sigma = \sigma_0\phi(t); \\ x \to \infty: \quad T = T_0, \quad C = C_0, \quad \sigma = 0; \\ t = 0: \quad C = C_0, \quad \sigma = 0, \quad C_P = C_{p0}; \quad T = T_0, \quad \frac{\partial C}{\partial t} = 0, \quad \frac{\partial \sigma}{\partial t} = 0; \end{gathered} \tag{18}$$

m_0, q_0, σ_0 are external influence parameters related to fluxes of particles, heat and stresses, respectively.

From (10), (11) and (14), (15), the second-order differential equations on both time and coordinate for the introduced impurity concentration and temperature follow:

$$\rho_0\left(\frac{\partial C}{\partial t} + t_D\frac{\partial^2 C}{\partial t^2}\right) = \frac{\partial}{\partial x}\left(\rho_0 D\frac{\partial C}{\partial x}\right) - \frac{\partial}{\partial x}\left(B_\sigma C\frac{\partial \sigma}{\partial x}\right) - \Phi - t_D\frac{\partial \Phi}{\partial t}; \tag{19}$$

$$t_q\rho_0 C_\sigma\frac{\partial^2 T}{\partial t^2} + \rho_0 C_\sigma\frac{\partial T}{\partial t} = \frac{\partial}{\partial x}\left(\lambda_T\frac{\partial T}{\partial x}\right) + Q\Phi + t_q Q\frac{\partial \Phi}{\partial t} - t_q\frac{\partial}{\partial t}\left(\alpha_T T\frac{\partial \sigma}{\partial t}\right) - \alpha_T T\frac{\partial \sigma}{\partial t}. \tag{20}$$

From (12) and (16) we find:

$$\frac{\rho_0}{E}\frac{\partial^2 \sigma}{\partial t^2} + \rho_0\alpha_T\frac{\partial^2 T}{\partial t^2} + \rho_0\left(\alpha - \alpha_0\right)\frac{\partial^2 C}{\partial t^2} + \rho_0\left(\alpha_P - \alpha_0\right)\frac{\partial^2 C_P}{\partial t^2} = \frac{\partial^2 \sigma}{\partial x^2}, \tag{21}$$

or

$$\rho_0\frac{\partial^2 u}{\partial t^2} = E\frac{\partial^2 u}{\partial x^2} - E\alpha_T\frac{\partial T}{\partial x} - E\left(\alpha - \alpha_0\right)\frac{\partial C}{\partial x} - E\left(\alpha_P - \alpha_0\right)\frac{\partial C_P}{\partial x}.$$

The last relation can be written in deformations:

$$\rho_0\frac{\partial^2 \varepsilon}{\partial t^2} = E\frac{\partial^2 \varepsilon}{\partial x^2} - E\alpha_T\frac{\partial^2 T}{\partial x^2} - E\left(\alpha - \alpha_0\right)\frac{\partial^2 C}{\partial x^2} - E\left(\alpha_P - \alpha_0\right)\frac{\partial^2 C_P}{\partial x^2}.$$

The kinetic equation (13) remains unchanged.

Note that, as in the classical theory of thermoelasticity [28, 29], the motion equation in stresses contains the temperature and concentration derivatives with time, and the motion equation in deformations contains temperature and concentration derivatives with the space coordinate.

3. Method for solving

By analogy with [16, 30], we introduce dimensionless variables for the presented equations system (19)-(21) with initial and boundary conditions (18):

$$\tau = \frac{t}{t_*}, \qquad \xi = \frac{x}{x_*}, \qquad S = \frac{\sigma}{\sigma_*}, \qquad \Theta = \frac{T - T_0}{T_* - T_0}, \qquad e = \frac{\varepsilon}{\varepsilon_*}.$$

The scales are defined by expressions: $t_* = x_* \sqrt{\rho_0 / E}$ is the time it takes the elastic wave to move the distance $x_* = \sqrt{t_* \lambda_T / (\rho_0 C_\sigma)}$ is the heating area formed during this time; $\sigma_* = E\alpha_T (T_* - T_0)$ is the maximum thermal stresses arising at heating to temperature T_*; $T_* = T_0 + \frac{q_0 x_*}{\lambda_T}$ is the temperature at depth x_* when the material is heated by a flux of value q_0, $\varepsilon_* = \alpha_T (T_* - T_0)$ is the maximum thermal strain achieved at heating to the temperature of T_*.

As a result, we have the equations system in dimensionless variables:

$$\frac{\partial^2 S}{\partial \tau^2} + \frac{\partial^2 \Theta}{\partial \tau^2} + \gamma \frac{\partial^2 C}{\partial \tau^2} + \gamma_P \frac{\partial^2 C_P}{\partial \tau^2} = \frac{\partial^2 S}{\partial \xi^2}, \tag{22}$$

$$\frac{\partial C}{\partial \tau} + \tau_D \frac{\partial^2 C}{\partial \tau^2} = \mathrm{Le} \frac{\partial}{\partial \xi}\left[F_{\mathrm{D}}(\Theta) f(C) \frac{\partial C}{\partial \xi} \right] - \frac{\omega \gamma M}{(\Theta + \chi)} C \,\mathrm{Le} \frac{\partial}{\partial \xi}\left[F_{\mathrm{D}}(\Theta) \frac{\partial S}{\partial \xi} \right] - \tau_{ch}\left[\psi(C) F_{ch}(\Theta) + \tau_D \frac{\partial \psi(C) F_{ch}(\Theta)}{\partial \tau} \right], \tag{23}$$

$$\tau_q \frac{\partial^2 \Theta}{\partial \tau^2} + \frac{\partial \Theta}{\partial \tau} = \frac{\partial^2 \Theta}{\partial \xi^2} - \tau_q \omega \frac{\partial}{\partial \tau}\left((\Theta + \chi) \frac{\partial S}{\partial \tau} \right) - \omega (\Theta + \chi) \frac{\partial S}{\partial \tau} + \Omega \tau_{ch}\left[\psi(C) F_{ch}(\Theta) + \tau_q \frac{\partial \psi(C) F_{ch}(\Theta)}{\partial \tau} \right], \tag{24}$$

$$\frac{\partial C_P}{\partial \tau} = \tau_{ch} \psi(C) F_{ch}(\Theta), \tag{25}$$

with initial and boundary conditions:

$$\xi = 0: \quad \mathbf{J} = \tilde{m}_0 \phi(\tau); \qquad \mathbf{J}_q = \tilde{q}_0 \phi(\tau); \qquad S = \tilde{\sigma}_0 \phi(\tau); \tag{26}$$

$$\xi \to \infty: \quad C = C_0; \qquad \Theta = 0; \qquad S = 0; \tag{27}$$

$$\tau = 0: \quad C = C_0; \qquad C_P = C_{P0}; \qquad S = 0; \qquad \Theta = 0; \qquad \frac{\partial C}{\partial \tau} = 0; \qquad \frac{\partial \Theta}{\partial \tau} = 0; \qquad \frac{\partial S}{\partial \tau} = 0, \tag{28}$$

where $F_D(\Theta) = \exp\left(\frac{1}{\beta_D} \frac{(\Theta - 1)}{(\Theta + \chi)} \right)$, $F_{ch}(\Theta) = \exp\left(\frac{1}{\beta_{ch}} \frac{\Theta - 1}{(\Theta + \chi)} \right)$ are dimensionless diffusion coefficients.

The fluxes of heat and mass in dimensionless form:

$$\mathbf{J} = -f(C) F_D(\Theta) \frac{\partial C}{\partial \xi} + \frac{\omega \gamma M C F_D(\Theta)}{(\Theta + \chi)} \frac{\partial S}{\partial \xi} - \tau_D \frac{\partial \mathbf{J}}{\partial \tau}, \tag{29}$$

$$\mathbf{J}_q = -\frac{\partial \Theta}{\partial \xi} - \tau_q \frac{\partial \mathbf{J}_q}{\partial \tau}. \tag{30}$$

All model parameters appearing in the system of equations (22)-(25) with conditions (26)-(28) and their physical meaning are presented in Table 1.

Table 1. Model parameters.

Parameter	Physical meaning
$\gamma = \frac{\Delta\alpha}{\alpha_T (T_* - T_0)}, \quad \gamma_P = \frac{\Delta\alpha_P}{\alpha_T (T_* - T_0)}$	Relationship of concentration strains to thermal strains for the introduced material and the chemical reaction product
$\tau_{ch} = t_* k_0 \exp\left(-\frac{E_0}{RT_*}\right)$	The ratio of the characteristic propagation time of mechanical disturbances to the characteristic time of the chemical reaction
$\Omega = \frac{Q_{ch}}{\rho C_\sigma (T_* - T_0)}$	The ratio of heat release in the reaction to the heat that is stored due to external heating to a temperature T_*
$\tau_q = \frac{t_q}{t_*}, \quad \tau_D = \frac{t_D}{t_*}$	Relative relaxation times of heat flux and mass flux
$\tilde{m}_0 = \frac{m_0}{J_{q^*}}, \quad \tilde{\sigma}_0 = \frac{\sigma_0}{\sigma_*}, \quad \tilde{q}_0 = \frac{q_0}{J_{q^*}}$	Dimensionless particle beam density, external mechanical action and external heat flux density
$\omega = \frac{E\alpha_T^2 (T_* - T_0)}{\rho C_\sigma}$	Coupling coefficient of thermal and mechanical fields
$\mathrm{Le} = \frac{D_0 \exp\left(-E_D/(RT_*)\right)}{\kappa_T}, \quad \kappa_T = \lambda_T/(C_\sigma \rho)$	The ratio of the diffusion coefficient at the characteristic temperature to the thermal diffusivity coefficient
$\chi = \frac{T_0}{(T_* - T_0)}, \quad \beta_{\mathrm{ch}} = \frac{RT_*}{E_0}, \quad \beta_{\mathrm{D}} = \frac{RT_*}{E_D}, \quad M = \frac{mC_\sigma}{R}$	Auxiliary parameters

For the obtained model parameters, based on the literature data [31], the estimation of acceptable ranges of numerical values for a wide class of metallic materials was carried out. The intervals of variation of the main parameters are given in Table 2. The table shows that many parameters change in a sufficiently large interval.

Table 2. Acceptable ranges of model parameters numerical values.

Parameter	Variation interval	Parameter	Variation interval	Parameter	Variation interval
$\gamma,\ \gamma_P$	$\left[-6\cdot10^{-2}...100\right]$	τ_D	$\left[0,025...2,5\right]$	ω	$\left[5\cdot10^{-5}...0,5\right]$
τ_{ch}	$\left[0,2\cdot10^{-26}...0,2\cdot10^{13}\right]$	$\tilde{m}_0$	$\left[25\cdot10^{-5}...200\right]$	Le	$\left[6\cdot10^{-22}...10^{-2}\right]$
Ω	$\left[0,7\cdot10^{-6}...200\right]$	$\tilde{\sigma}_0$	$\left[0,02\cdot10^{-5}...10\right]$	β_{ch}	$\left[0,03...0,3\right]$
τ_q	$\left[0,25\cdot10^{-2}...0,25\right]$	$\tilde{q}_0$	$\left[3\cdot10^{-11}...7\right]$	β_{D}	$\left[0,02...0,06\right]$

The system (22)-(25) with conditions (26)-(28) was solved numerically using an implicit symmetric second-order difference scheme to represent the derivatives both with time and with

coordinate. The coefficients in the derivatives were calculated owing to the values from the previous layer over time. The convergence was investigated by calculations with decreasing of the grid step (increasing the number of partitions of the computational domain) and decreasing of the time step. For example, the first summand in the right part of the diffusion equation (23) after approximation had the form:

$$\frac{\partial}{\partial\xi}\left[F_{\mathrm{D}}(\Theta)\,f(C)\frac{\partial C}{\partial\xi}\right]\to$$

$$\frac{1}{\Delta\xi}\left[\frac{F_{\mathrm{D}}\left(\overset{\vee}{\Theta}_{i+1}\right)f\left(\overset{\vee}{C}_{i+1}\right)+F_{\mathrm{D}}\left(\overset{\vee}{\Theta}_{i}\right)f\left(\overset{\vee}{C}_{i}\right)}{2}\frac{C_{i+1}-C_i}{\Delta\xi}-\frac{F_{\mathrm{D}}\left(\overset{\vee}{\Theta}_{i-1}\right)f\left(\overset{\vee}{C}_{i-1}\right)+F_{\mathrm{D}}\left(\overset{\vee}{\Theta}_{i}\right)f\left(\overset{\vee}{C}_{i}\right)}{2}\frac{C_i-C_{i-1}}{\Delta\xi}\right].$$

The second summand (without coefficients) was completely dissected through the values from the previous layer over time:

$$\frac{C}{(\Theta+\chi)}\frac{\partial}{\partial\xi}\left[F_{\mathrm{D}}(\Theta)\frac{\partial S}{\partial\xi}\right]\to$$

$$\frac{\overset{\vee}{C}_i}{\left(\overset{\vee}{\Theta}_i+\chi\right)}\frac{1}{\Delta\xi}\left[\frac{F_{\mathrm{D}}\left(\overset{\vee}{\Theta}_{i+1}\right)+F_{\mathrm{D}}\left(\overset{\vee}{\Theta}_{i}\right)}{2}\frac{\overset{\vee}{S}_{i+1}-\overset{\vee}{S}_i}{\Delta\xi}-\frac{F_{\mathrm{D}}\left(\overset{\vee}{\Theta}_{i-1}\right)+F_{\mathrm{D}}\left(\overset{\vee}{\Theta}_{i}\right)}{2}\frac{\overset{\vee}{S}_i-\overset{\vee}{S}_{i-1}}{\Delta\xi}\right].$$

When constructing a discrete analogue of the thermal conductivity equation,variants are possible giving the numerically same results: 1. The time derivatives of stresses are taken from the previous time layer. 2. The second derivative of stresses is replaced with expression from the motion equation, and the emerging second derivative of concentrations is replaced with expression from the diffusion equation. Then all derivatives not of the temperature are represented in the same way as on the bottom layer. Variant 1 turned out to be more stable.

So, the time derivatives of temperature were approximated as follows:

$$\frac{\partial^2\Theta}{\partial\tau^2}\to\frac{\overset{\wedge}{\Theta}_i-2\Theta_i+\overset{\vee}{\Theta}_i}{\Delta\tau^2};\qquad\frac{\partial\Theta}{\partial\tau}\to\frac{\overset{\wedge}{\Theta}_i-\Theta_i}{\Delta\tau}.$$

The source summands were taken from the previous time layer:

$$\frac{\partial\psi(C)F_{ch}(\Theta)}{\partial\tau}=F_{ch}(\Theta)\frac{\partial\psi(C)}{\partial\tau}+\psi(C)\frac{\partial F_{ch}(\Theta)}{\partial\tau}=F_{ch}(\Theta)\left[(1-2C-C_P)\frac{\partial C}{\partial\tau}-C\tau_{ch}\psi(C)F_{ch}(\Theta)\right]+$$

$$+\psi(C)\exp\left(\frac{1}{\beta_{ch}}\frac{\Theta-1}{(\Theta+\chi)}\right)\frac{1}{\beta_{ch}}\frac{\chi+1}{(\Theta+\chi)^2}\frac{\partial\Theta}{\partial\tau}.$$

The two similar variants of the motion equation approximation giving similar results are possible. As a result, all equations were linearized and "decoupled" and could be solved numerically independently of each other and in any convenient way. In the present work, all equations were reduced to a form suitable for the sweep method.

The boundary conditions were also written in discrete form using difference schemes with the second order of approximation. For this purpose, we used Taylor series expansions of the functions in the nodes of the difference mesh nearest to the boundary, relative to the values at the boundary points up to the values of the second order of smallness. The second derivatives appearing in the expansion were found from the basic differential equations, which are also correct at the boundary points.

The kinetics equation was represented as:

$$\frac{\hat{C}_P - C_P}{\Delta\tau} = \tau_{ch} \exp\left(\frac{1}{\beta_{ch}} \frac{\Theta - 1}{(\Theta + \chi)}\right) C\left[1 - C - \hat{C}_P\right],$$

from which

$$\hat{C}_P = \frac{C_P + \Delta\tau \cdot \tau_{ch} F_{ch}(\Theta) C[1 - C]}{1 + \Delta\tau \cdot \tau_{ch} F_{ch}(\Theta) \cdot C}.$$

Note that the kinetic equation is solved "last", therefore the diffusant concentration and the temperature in it are already found at this time layer. This approach has proven itself well in solving problems in macrokinetics.

The solutions converged to a certain limit when the values of the mesh parameters were decreased. The mesh refinement and reduction of the time step ended when the results stopped varying up to 3-5%. The worst convergence was observed for the diffusion equation. The solution of the problem without taking into account the chemical reaction was in agreement with the solutions obtained in the previous author's work [16].

In general, there is no universal way to solve nonlinear coupled problems numerically, and there is no exact theory of the convergence and stability of the corresponding difference methods. Limitations in the solution of coupled problems also apply to the numerical values of physical parameters. They are caused by the condition of non-negativity of the Onzager coefficient matrix. Negative concentrations and other non-physical effects can occur if it is not taken into account. This problem is known in chemical kinetics, but is rarely discussed in literature devoted to the numerical methods.

4. Results and discussion

It is necessary to consider in detail the dynamics of propagation of strain/stress waves, thermal and concentration waves at different time intervals in the study of the interdependence of these processes. In the presented formulation of the problem, they are defined by the following parameters: the characteristic time of the pulse action τ_{imp} and the relaxation times for diffusion τ_D and thermal conductivity τ_q. In this case, their values are correlated as follows: $\tau_q < \tau_D < \tau_{imp}$.

Table 3. Calculated values of model parameters.

Parameter	Value	Parameter	Value	Parameter	Value	Parameter	Value
γ	1,5	Ω	200,0	ω	0,05	M	10,5
γ_P	–0,5	τ_D	0,02	τ_q	0,005	τ_{imp}	0,03
$\tilde{m}_0$	5,0	$\tilde{\sigma}_0$	0,001	$\tilde{q}_0$	5,0	χ	0,55
τ_{ch}	200,0	Le	0,0025	β_D	0,027	β_{ch}	0,3

Since the areas of variation of many model parameters are significant, it depends on both the type of specific materials and processing conditions, so a parametric study is of interest. The value

of some parameters was fixed. The numerical values of the model parameters for the calculations were taken without connection to real materials. This is partly due to the fact that many of the physical parameters included in the dimensionless complexes are known with a large inaccuracy or the data on it are not reliable and depend on the model on the basis of which they were estimated. The values used in this paper are given in Table 3.

We assume that a single sinusoidal pulse acts on the surface of the target:

$$\phi(\tau)=\begin{cases}\sin\left(\dfrac{\pi\tau}{\tau_{imp}}\right), & \tau\le\tau_{imp},\\ 0, & \tau>\tau_{imp}.\end{cases}$$

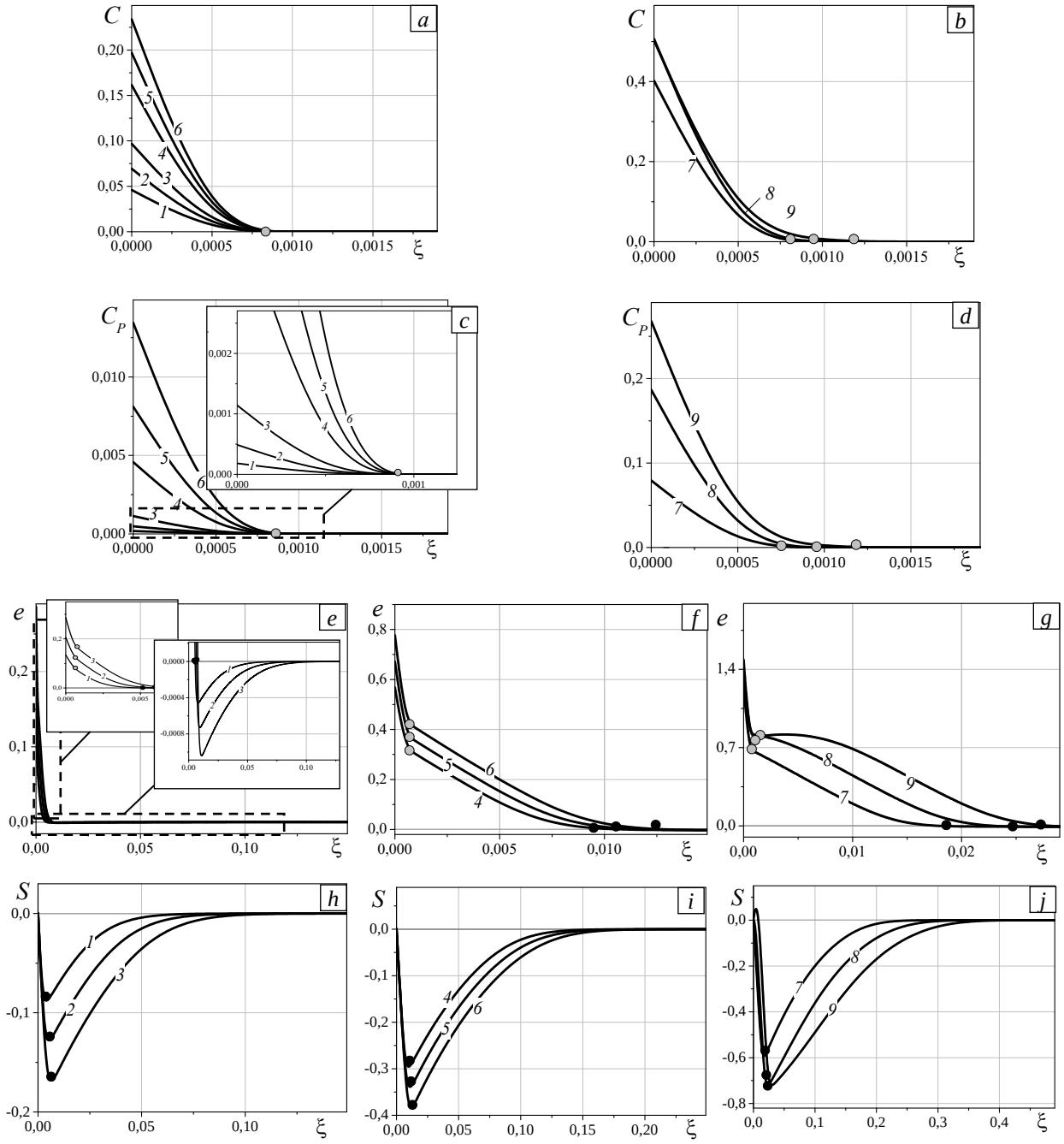

Fig. 1. The results of solving a coupled problem: distribution of introduced material concentration (*a*, *b*), mass content of the reaction product (*c*, *d*), strain (*e*–*g*), stress (*h*–*j*) at different time moments τ : *1* – 0,004; *2* – 0,005; *3* – 0,006; *4* – 0,008; *5* – 0,009; *6* – 0,01; *7* – 0,015; *8* – 0,02; *9* – 0,025; fragments of graphs that are presented in a larger scale are marked with a dotted line.

Figure 1 shows the results of solving the problem for different time intervals. It can be seen that in the concentration wave (Fig. 1 a, b) there are no visible distortions associated with the influence of thermal and mechanical waves for the selected parameters set. Diffusion wave propagates much slower than mechanical disturbances. The velocity of the stress, strain and temperature waves are close, however, the leading front of the strain wave is only visible in the graphs after zooming (Fig. 1 e). The following figures in the article show only part of the deformation wave at the left boundary, which shows the mutual influence of waves of different physical nature. Because the wave velocities are different, there is no change at the leading edge of the mechanical wave. By the time $\tau \le \tau_{imp}$ (Fig. 1a, b) the depth of implanted impurity penetration increases from $\approx 0,8 \cdot 10^{-3}$ to $\approx 1,2 \cdot 10^{-3}$. The chemical reaction starts almost immediately at $\tau \approx \tau_q$, but the concentration of the reaction product at the initial moments is insignificant: $C_P \approx 1,8 \cdot 10^{-4}$ (Fig. 1 c).

From the time $\tau < \tau_q$, we can see some distortion on the strain wave that corresponds to the position of the leading front of the impurity concentration wave (Fig. 1 e-g, gray circles). The place where the deformation wave crosses the axis $O\xi$ is marked with black circles, that is, the sign of the deformation changes here. There is an extreme on the stress wave in this area (Fig. 1 h-j, black circles). Up to the time $\tau = 0,02$ (equal to τ_D), the concentration of the impurity on the left boundary increases, but then begins to decrease, which is explained by a rapid increase in the reaction product concentration (Fig. 1 b, d).

At moments of time 1-9, when $\tau < \tau_{imp}$ (Fig. 1 h-j, Fig. 2 a), any features do not appear on the temperature and stress waves. But by the time $\tau = \tau_{imp}$ and for times slightly longer than the pulse action time (Fig. 2 b, curves 10-12), the formation of a maximum is observed on the thermal wave (gray squares, which correspond to distortions in the stress wave (Fig. 3 f)). For later moments of time (Fig. 2 b, curves 13-15), the temperature distribution does not have any pronounced extremes; a similar picture can be seen for the stress wave (Fig. 3 g).

Because the parameter Ω in this paper is chosen sufficiently large, then the chemical reaction proceeds as long as there is an introduced impurity. After the pulse ends, product formation continues until the reaction rate becomes close to zero as a result of temperature decrease. The impurity concentration at the left boundary decreases from 42% to 7% at the time interval $\tau = [0,03...0,07]$ (Fig. 3 a). By the time $\tau = 0,07$ maximum value of C is located at some distance from the treated surface and the extreme in the strain wave corresponds to it (Fig. 3 c, area in a larger scale). As noted, the gray circles illustrate the mutual influence of concentration and strain waves. These points are the end points on the graph for the impurity concentration for each time moment. So the strain wave to the right of these selected points propagates independently of C. For moments of time $\tau \ge \tau_D$ (more pronounced near time $\tau = \tau_{imp}$), we can see additional extremes on the stress and strain waves, which correspond to each other (Fig. 3 b, f, white circles).

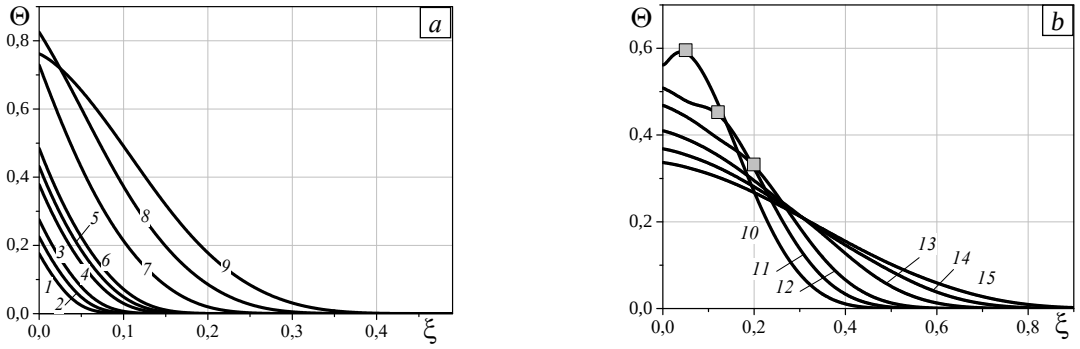

Fig. 2. Temperature distribution at different time moments τ : *1* – 0,004; *2* – 0,005; *3* – 0,006; *4* – 0,008; *5* – 0,009; *6* – 0,01; *7* – 0,015; *8* – 0,02; *9* – 0,025; *10* – 0,03; *11* – 0,035; *12* – 0,04; *13* – 0,05; *14* – 0,06; *15* – 0,07.

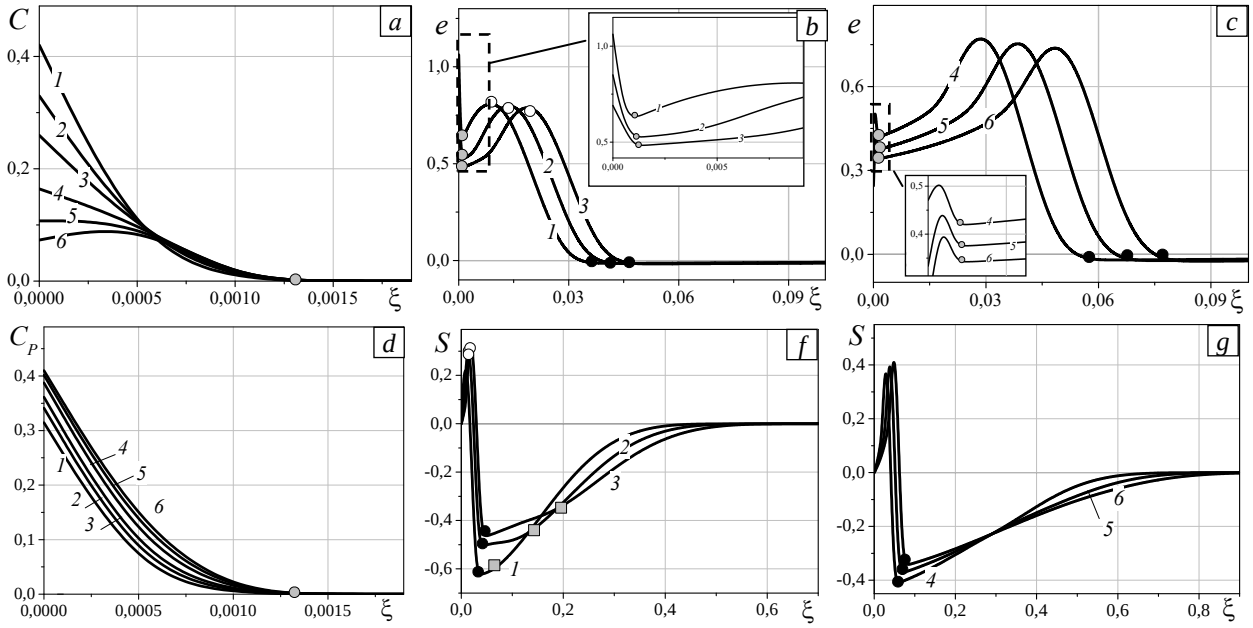

Fig. 3. The results of solving a coupled problem: distribution of introduced material concentration (*a*), strain (*b*, *f*), mass content of the reaction product (*d*), stress (*c*, *g*) at different time moments τ : *1* – 0,03; *2* – 0,035; *3* – 0,04; *4* – 0,05; *5* – 0,06; *6* – 0,07.

The parameters responsible for the chemical reaction in the problem are Ω, τ_{ch}, β_{ch}. Figure 4 shows the effect of heat release Ω in the reaction on the distributions of the studied quantities. It can be seen that the increase Ω leads to an increase in the mass content of the reaction product, consequently, the introduced impurity concentration decreases, the temperature increases, and the stresses and strain increase in the extreme regions, but near the treated surface, the strains are lower due to a decrease in the impurity concentration (Fig. 4 d, area on a larger scale).

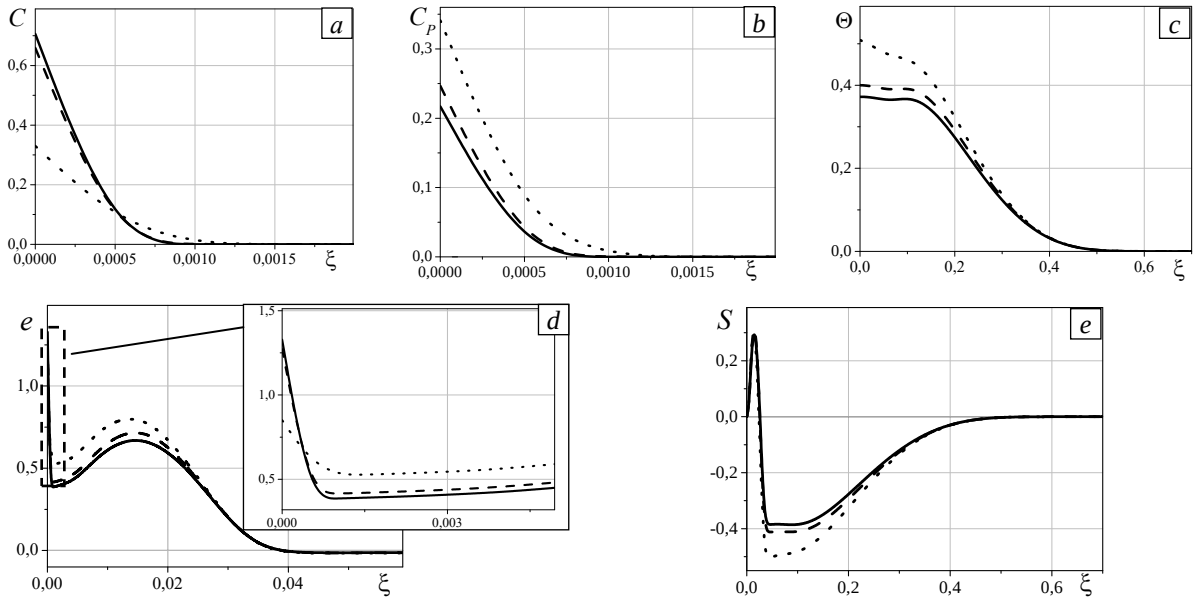

Fig. 4. Influence of the parameter Ω value. Distribution of introduced material concentration (*a*), mass content of the reaction product (*b*), temperature distribution (*c*), strain (*e*), stress (*d*) at different values of Ω: 10,0 (solid line); 100,0 (dashed line); 200,0 (dotted line); time moment $\tau = 0,035$.

At a small value of Ω, for example $\Omega = 10$ (Fig. 4, solid line), the chemical reaction proceeds as long as the temperature rises due to the input energy. Then there is not enough heat to continue the reaction. Thus, by the time $\tau = \tau_{imp}$ the distribution C_P takes its final form, the reaction stops.

The increasing parameter values τ_{ch}, β_{ch} also leads to increase the reaction product concentration, temperature, strains and stresses and the impurity concentration decreases. The parameter τ_{ch} has a very strong influence on the value of mass content of product. If the value of this parameter is small, then value of C_P also becomes insignificant. In this case, even the maximum heat release parameter in the reaction Ω does not lead to visible changes in the graphs of temperature, strains, stresses, and impurity concentration, i.e., the slow formation of the product in the reaction will have almost no effect on their distribution.

6. Conclusion

Thus, the paper presents a coupled non-isothermal model of the process of material introduction into the target surface under conditions of surface treatment by a particle flux. The model takes into account the interaction of different-scale processes: impurity diffusion, heat propagation, and mechanical disturbances. In addition, it involves chemical interaction between the introduced impurity and the substrate material during processing. It was found that the interrelation of these processes leads to the appearance of distortion of the mechanical wave. There is a maximum in the temperature wave at some distance from the treated surface at times close and comparable to the pulse action time; in this time interval, the temperature in the depth of the target is higher than on the surface. The impurity concentration distribution shows no visible distortions, but, like the heat flux, it has a wave character. Note that the chosen set of model parameters is of great importance, and perhaps a different combination of them will reveal new, or strengthen already known, interactions of the considered processes. The area of variation of the parameters depends not only on the properties of the materials and chemical reaction conditions, but also on the processing regime.

The work was supported by RFBR and ROSATOM, grant No 20-21-00064.

References

1. Kolesnikov V.I., Kudryakov O.V., Zabiyaka I.Yu., Novikov E.S., Manturov D.S. Structural aspects of wear resistance of coatings deposited by physical vapor deposition. *Phys. Mesomech.*, 2020, vol. 23, pp. 570-583. https://doi.org/10.1134/S1029959920060132
2. Panin V.E., Narkevich N.A., Durakov V.G., Shulepov I.A. Control over the structure and wear resistance of an electron beam overlay coating of carbon-nitrogen austenitic steel. *Fiz. mezomekh. – Physical mesomechanics*, 2020, vol. 23, no. 2, pp. 15-23. https://doi.org/10.24411/1683-805X-2020-12002
3. Byeli A.V., Kukareko V.A., Kononov A.G., Bilenko E.G. Structure transformations and amorphization of Fe-Zr alloy under irradiation with nitrogen ion intense flows. *J. Synch. Investig.*, 2008, vol. 2, pp. 340-343. https://doi.org/10.1134/S1027451008030026
4. Kurzina I.A., Popova N.A., Nikonenko E.L., Kalashnikov M.P., Savkin K.P., Sharkeev Yu.P., Kozlov E.V. Influence of the irradiated dose on structural state and phase composition of surface layers ultrafine-titanium. *Izv. vuzov. Fizika – Russian Physics Journal*, 2014, vol. 57, no. 7-2, pp. 74-78.
5. Vershinin G.A., Grekova T.S., Gering G.I., Kurzina I.A., Sharkeev Yu.P. Analysis of concentration field formation in titanium under aluminum ion implantation via a gas-and-metal film deposited on a target surface. *J. Synch. Investig.*, 2012, vol. 6, pp. 251-254. https://doi.org/10.1134/S1027451012030226
6. Valyayev A.N. *Modifikatsiya svoystv materialov i sintez tonkikh plenok pri obluchenii intensivnymi elektronnymi i ionnymi puchkami* [Modification of material properties and synthesis of thin films by irradiation with intense electron and ion beams]. Ust-Kamenogorsk, VKTU, 2000. 345 p.
7. Uglov V.V., Cherenda N.N., Anishchik V.M., Astashinskiy V.M., Kvasov N.T. *Modifikatsiya materialov kompressionnymi plazmennymi potokami* [Modification of materials by compressive plasma flows]. Minsk, BGU, 2013. 248 p.

8. Zhmakin A.I. Heat conduction beyond the Fourier law. *Tech. Phys.*, 2021, vol. 66, pp. 1-22. https://doi.org/10.1134/S1063784221010242
9. Babenkov M.B., Ivanova E.A. Analysis of the wave propagation processes in heat transfer problems of the hyperbolic type. *Continuum Mech. Thermodyn.*, 2014, vol. 26, pp. 483-502. https://doi.org/10.1007/s00161-013-0315-8
10. Babenkov M.B. Propagation of harmonic perturbations in a thermoelastic medium with heat relaxation. *J. Appl. Mech. Tech. Phy.*, 2013, vol. 54, pp. 277-286. https://doi.org/10.1134/S0021894413020132
11. Knyazeva A.G. Nonlinear diffusion models of deformed media. *Fiz. mezomekh. – Physical mesomechanics*, 2011, vol. 14, no. 6, pp. 35-51.
12. Chepak-Gizbrekht M.V., Knyazeva A.G. Influence of thermal diffusion on the redistribution of elements and mechanical stresses during metal surface treatment with a particle beam. *Izv. vuzov. Fizika – Russian Physics Journal*, 2013, vol. 56, no. 12-2, pp. 39-45.
13. Knyazeva A.G., Han A. Intermetallic phases formation at the conditions of ion implantation. *Izv. vuzov. Fizika – Russian Physics Journal*, 2015, vol. 58, no. 6-2, pp. 126-130.
14. Davydov S.A., Zemskov A.V., Tarlakovskii D.V. Surface Green's function in non-stationary problems of thermomechanical diffusion. *PPP – The Problems of Strength and Plasticity*, 2017, vol.79, no. 1, pp. 38-47.
15. Vestyak A.V., Zemskov A.V., Tarlakovskii D.V. Two-dimensional unsteady problem of elasticity with diffusion for orthotropic one-component half-plane. *PPP – The Problems of Strength and Plasticity*, 2016. vol. 78, no. 1, pp. 13-21.
16. Parfenova E.S., Knyazeva A.G. Non-isothermal mechanodiffusion model of the initial stage of penetration of particle flow in a target surface. *Vychisl. mekh. splosh. sred – Computational continuum mechanics*, 2019. vol. 12, no. 1, pp. 36-47. https://doi.org/10.7242/1999-6691/2019.12.1.4
17. Nowacki W. Dynamical problems of thermodiffusion in solids. Part I. *Bull. Acad. Pol. Sci. Ser. Sci. Technol.*, 1974, vol. 22, pp. 55-64.
18. Nowacki W. Dynamical problems of thermodiffusion in solids. Part II. *Bull. Acad. Pol. Sci. Ser. Sci. Technol.*, 1974, vol. 22, pp. 129-135.
19. Nowacki W. Dynamical problems of thermodiffusion in solids. Part III. *Bull. Acad. Pol. Sci. Ser. Sci. Technol.*, 1974, vol. 22, pp. 257-266.
20. Nowacki W. Dynamical problems of thermodiffusion in elastic solids. *Proc. Vib. Probl.*, 1974. vol. 15, pp. 105-128.
21. Sherief H.H., Hamza F., Saleh H. The theory of generalized thermoelastic diffusion. *Int. J. Eng. Sci.*, 2004, vol. 42, pp. 591-608. https://doi.org/10.1016/j.ijengsci.2003.05.001
22. Aouadi M. Generalized theory of thermoelastic diffusion for anisotropic media. *J. Therm. Stresses*, 2008, vol. 31, pp. 270-285. https://doi.org/10.1080/01495730701876742
23. Knyazeva A.G. Diffuziya i reologiya v lokal'no-ravnovesnoy termodinamike [Diffusion and rheology in locally-equilibrium thermodynamics]. *Vestnik PGTU. Matematicheskoye modelirovaniye sistem i protsessov – PNRPU Mechanics Bulletin*, 2005, no. 13, pp. 45-60.
24. Sedov L.I. *Mekhanika sploshnoy sredy. T. 1* [Continuum mechanics. Vol. 1]. Moscow, Nauka, 1970. 492 p.
25. Aouadi M. A theory of thermoelastic diffusion materials with voids. *Z. Angew. Math. Phys.*, 2010, vol. 61, pp. 357-379. https://doi.org/10.1007/s00033-009-0016-0
26. Aouadi M. Theory of generalized micropolar thermoelastic diffusion under Lord-Shulman model. *J. Therm. Stresses*, 2009, vol. 32, pp. 923-942. https://doi.org/10.1080/01495730903032276
27. Elhagary M.A. Generalized thermoelastic diffusion problem for an infinitely long hollow cylinder for short times. *Acta Mech.*, 2011, vol. 218, pp. 205-215. https://doi.org/10.1007/s00707-010-0415-5
28. Nowacki W. *Dynamiczne zagadnienia termosprężystości* [Dynamical problems of thermoelasticity]. Warzawa, 1966. 366 p.
29. Podstrigach Ya.S., Kolyano Yu.M. *Obobshchennaya termomekhanika* [Generalized Thermomechanics]. Kiev, Naukova dumka, 1976. 311 p.
30. Il'ina E.S., Demidov V.N., Knyazeva A.G. The modeling features of diffusion processes in elastic body under particles surface treatment. *Vestnik PNIPU. Mekhanika – PNRPU Mechanics Bulletin*, 2012, no. 3, pp. 25-49.
31. Grigor'yev A.S., Meylikhov K.Z. (ed.) *Fizicheskiye velichiny: Spravochnik* [Physical quantities: Handbook]. Moscow, Energoatomizdat, 1991. 1232 p.

The authors declare no conflict of interests.
The paper was received on 04.03.2021. The paper was accepted for publication on 29.03.2021.